Molecular Simulation, Vol. 31, Nos. 6–7, 15 May – 30 May 2005, 457–463

Taylor & Francis
Taylor & Francis Group

Local density profiles are coupled to solute size and attractive potential for nanoscopic hydrophobic solutes

N. CHOUDHURY† and B. MONTGOMERY PETTITT*

Department of Chemistry, University of Houston, Houston, TX 77204-5003, USA

(Received November 2004; In final form December 2004)

We employ constant pressure molecular dynamics simulations to investigate the effects of solute size and solute–water dispersion interactions on the solvation behavior of nanoscopic hydrophobic model solutes in water at normal temperature and pressure. The hydration behavior around a single planar atomic model solute as well as a pair of such solutes have been considered. The hydration water structure of a model nanoscopic solute with standard Lennard-Jones interaction is shown to be significantly different from that of their purely repulsive analogues. The density of water in the first solvation shell of a Lennard-Jones solute is much higher than that of bulk water and it remains almost unchanged with the increase of the solute dimensions from one to a few nanometers. On the other hand, for a purely repulsive analogue of the above model, solute hydration behavior shows a marked solute size dependence. The contact density of water in this case decreases with the increasing dimension of the solute. We also demonstrate the effect of solute–solvent attraction on the cavity formation in the inter solute region between two solutes with an inter solute separation of 6.8 Å, corresponding to the first solvent separated minimum in the free energy profile as obtained in our earlier work.

Keywords: Hydrophobic hydration; Dewetting; NPT molecular dynamics simulation

1. Introduction

Hydrophobicity has long been recognized [1–6] as a central phenomenon in the fields of solvation physics, chemistry, biochemistry and biology. Understanding the nature of the interface between a hydrophobic solute and water holds the key to the understanding of a large variety of phenomena as diverse as protein folding [7,8], self-assembly [9,10] of amphiphiles, lipid aggregation, and the self-assembly of hydrophobic nano materials [11,12] such as carbon nano tubes. Water is a peculiar solvent [13] due to its many anomalous properties, which are believed to be the consequence of the hydrogen-bond network present in water. Dissolution of any hydrophobic substance in water is thought to cause [14] an energy loss due to the disruption of this hydrogen bond network. It is well understood [14–18] that water molecules reorganize themselves around a small hydrophobic solute without grossly disturbing the hydrogen bond network, as a small solute can easily be accommodated in any of the natural atomic sized cavities present in bulk water. However dissolution and stability of a nanoscopic solute, which is much larger than the size of a spontaneous and probable cavity present in water, are not possible by this mechanism and therefore understanding the solvation of large solute in water has been the subject matter of many recent studies [14,19–34] and much debate [35].

In theoretical and computational studies of hydrophobic hydration, it is often useful to consider simplified models. The simplest of such model for hydrophobic solute is a hard body with purely repulsive interactions. This simplified model has been used in many recent theoretical [14,17,21] and computational [25,36] studies of hydrophobic hydration. It has been observed [23,25,26] in some of these studies with nanoscopic purely repulsive model solutes in water that all the water molecules have been expelled from the inter solute region when two solutes are brought closer than a certain critical distance, creating a vapor phase or bubble in the inter solute region, thereby causing a collapse of the two solutes. Incorporation of very weak solute–solvent attractive interactions in an idealized manner without taking into account the atomistic

*Corresponding author. Fax: +1-713-743-2709. E-mail: pettitt@uh.edu
†On leave from RC & CD Division, Bhabha Atomic Research Centre, Mumbai 400 085, India.

Molecular Simulation
ISSN 0892-7022 print/ISSN 1029-0435 online © 2005 Taylor & Francis Group Ltd
http://www.tandf.co.uk/journals
DOI: 10.1080/08927020500035457

nature and surface morphology of such solutes causes [22,26] the cavitation and dewetting effect to decrease although not completely diminished.

However, using an atomistic model for methane cluster, it has been shown [37] that wetting at a methane cluster–water interface is favorable when a realistic Lennard-Jones (LJ) potential is used to model individual methane molecule, although dewetting is associated with its hard sphere analogue. In this study no attempt was made to investigate the role of solute–solvent attraction on the dewetting in the inter solute region between two such solutes in terms of free energy of hydration. In a very recent study [38], considering flat plate-like nanoscopic solutes with atomistic detail, we have calculated the free energy of hydration as a function of the surface to surface distance and shown that mechanism of the contact pair formation depends on the nature of solute–solvent interaction. When the solute is modeled as a graphite-like plate made up of sp^2 carbon atoms with a reasonable dispersion interaction parameter, a cumulative effect of a large number of small attractive interactions between the solute atoms and water stabilizes the solvent separated state containing as little as one layer of water molecules between the two large solutes without any cavitation or drying. Although the dissolution process of a large hydrophobic solute in water is unfavorable, in general, due to the change in entropic–enthalpic compensation, a delicate balance [38] between solute–solvent and solute–solute attractive interaction and lost hydrogen bond energy with a sharp and shifted distribution of the binding energy of water [27] at higher energy apparently determine the stability of such a contact pair state. This behavior is consistent with what has been observed in case of carbon nanotubes in water [27–29]. Using atomistic model of a carbon nanotube, Hummer *et al.* have demonstrated [27,28] that water not only hydrates the outer surface of the nano tube but also enters a very narrow pore inside the nanotube that can accommodate only a single file of water molecules. Thus it seems loss of hydrogen bonding does not prevent wetting of insoluble systems alone.

The attractive forces among the water molecules are unbalanced [37] in the region near a large repulsive solute due to the net loss of the favorable interactions in this region as compared to bulk. An effective repulsive potential—the cavity expulsion potential (CEP) [24] arises between the water and the solute surface due to this net attraction of the water molecules in the bulk as compared to the interfacial region. The CEP increases with increasing sizes of the solute because of the increase in unfavorable interactions with larger interfacial region. However, if there is an attractive interaction between a water molecule and the solute, the stabilizing effect of this solute–solvent attraction may offset the CEP. As discussed earlier [24,37], the attractive solute–solvent interaction acts in the opposite direction of CEP when solute size is varied. Therefore, an attractive solute–solvent interaction is a critical determinant of the dewetting behavior of a hydrophobic solute. In fact, the attractive solute–solvent interactions have been shown [24,37] to offset the CEP. As even the most hydrophobic regions in a protein have significant polarity and dispersion interactions, it may be misleading to extrapolate the cavitation and collapse seen [22,23,25,26] in the idealized model solutes to hydrophobicity induced protein folding and aggregation. In fact, in a recent computation study of protein folding [39], the water expulsion mechanism has not been observed.

In the present study we extend our previous investigation [38] to the hydration of a single nanoscopic solute. A comparison of the effect of solute size on the water structure around two model solutes with LJ and repulsive interactions has been made. We also examine the role of the van der Waals' attraction on the inter solute dewetting at a inter solute distance of 6.8 Å corresponding to a solvent separated state with a monolayer of water between two nanoscopic solutes as observed earlier [38].

2. Method

We shall first briefly recall the procedure used previously [38]. MD simulations are used to investigate the hydration structure around a single planar nanoscopic solute of various sizes and attractive strengths. Each of the hydrophobic solutes considered here was modeled as a single graphite-like sheet or plate made up of carbon atoms placed in the hexagonal lattice with carbon–carbon bond lengths of 1.4 Å. As earlier, the water molecule in this study also was represented by the standard SPC/E [40] model. In the single solute case, three solute sizes have been considered: (a) the smallest one is made up of 28 carbon atoms with a dimension of 7.4 Å × 7.1 Å, (b) an intermediate one is made up of 60 carbon atoms with the dimension of 11.1Å × 12.1 Å and (c) the largest one consists of 180 carbon atoms with the dimension of 21 Å × 20.7 Å. The numbers of water molecules in which three solutes have been solvated are 997, 1787 and 1700 for small, medium and large solutes, respectively. In each case at least two kinds of solute–solvent interaction have been considered, namely the usual LJ interaction with the parameters taken from AMBER force field [41] for the sp^2 carbon atom and the repulsive part of the same LJ potential as obtained using WCA splitting scheme [42]. Other studies in selected cases used a variety of well depth parameters. The plate in each case is placed in the middle of the box parallel to the *xy*-plane of the box.

We also investigate the effect of attractive solute–solvent interactions in the inter solute region at a fixed inter solute distance of 6.8 Å corresponding to the first solvent separated minimum of the free energy profile between two of the 60 carbon atom sheets studied earlier [38]. In this case, the two sheets of 11.1 Å × 12.1 Å dimension were placed symmetrically around the center of a cubic box containing 1800 water molecules, with the plates being parallel to each other as well as to the *xy*-plane with a fixed inter solute distances $r_0 = 6:8$ Å. Four different interaction parameters have been used for the solute potential in this case, namely

(1) a carbon–carbon LJ well depth $\epsilon_{CC} = 0.086\,\text{kcal mol}^{-1}$ (or $0.3598\,\text{kJ mol}^{-1}$), corresponding to the sp^2 carbon atoms in the AMBER force field [41], the same used by Hummer *et al*. [27] which we call system A (2) $\epsilon_{CC} = 0.052\,\text{kcal mol}^{-1}$ (or $0.2177\,\text{kJ mol}^{-1}$), (system B) (3) $\epsilon_{CC} = 0.023\,\text{kcal mol}^{-1}$ (or $0.0967\,\text{kJ mol}^{-1}$), (system C) (4) repulsive part of potential (1) split according to WCA scheme (system D). The usual Lorentz-Berthelot mixing rules were employed to calculate the interaction parameters for solute–water interactions. The solutes were kept fixed during the simulation.

Simulations in the isothermal isobaric (NPT) ensemble were carried out using the molecular dynamics (MD) extended system approach of Nose' and Anderson [43–45]. Periodic boundary conditions were applied and all electrostatic interactions were calculated using the Ewald method [46]. The bonds and angles between oxygen and hydrogen atoms of the water molecules were constrained by use of the RATTLE algorithm [46,47] and the solutes were kept rigid. All the systems were simulated at a target pressure of 1 atom and a target temperature of 298 K. The equations of motion were integrated using velocity Verlet algorithm [46,48] with a 2 fs time step. Each of these systems was equilibrated for 100 ps and structural properties were calculated from the coordinates saved for next 400 ps for one solute cases and 900 ps for two solute cases.

3. Results and discussions

For reference, the potentials of mean forces (PMFs), $w(r)$s, as a function of the separation between the two nanoscopic (60 atoms) parallel plates as calculated in our earlier study [38] with and without attractive solute–solvent interaction are shown in figure 1 as solid and dashed lines, respectively. In the inset (a) we show PMF as well as two components of it namely, solute–solute interaction potential and solvent induced part of the PMF for solute with attractive solute–solvent interaction and in inset (b) we show the same for the solute with purely repulsive interaction. The difference in the implied mechanism for the hydrophobic effect is profound. For the attractive plates we find a small solvent stabilization near contact (see the solvent induced PMF as shown by dashed line in the inset (a)) with the overall PMF (solid line) dominated by the solute–solute attractive potential (open circle with line). For the repulsive solute–solvent system we find a large, purely solvent induced stabilization near contact. For attractive solute–solvent interaction, another interesting feature in the PMF is the existence of the minimum around the inter solute distance of 6.8 Å, which is shown [38] to correspond to the solute–solvent configuration with a single layer of water molecule trapped between two solutes. This solvent separated state is nonexistent in the purely repulsive solute case even doubling the space between.

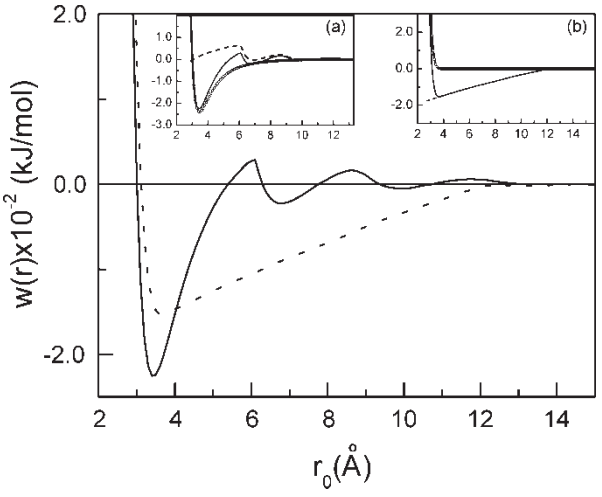

Figure 1. The potential of mean forces $w(r)$s for two nanoscopic carbon plates with two kinds of model potentials. The solid line is for a usual slightly attractive Lennard-Jones model of the solute atoms and the dashed line is for a purely repulsive model. In the insets (a) and (b) we show the solute-solute potential contribution (open circles with line) and solvent contribution (dashed line) to the potential of mean force (solid line) for attractive and repulsive solutes, respectively.

Expulsion of water structured by weak attractive forces leads to significant barriers in the approach of two solutes toward each other reminiscent of surface force experiments [49]. Studies on the effect of attractive solute–solvent interactions on this monolayer water state are reported in Section 3.2. We now consider the effect of solute sizes and solute–solvent attraction on the solvation structure of a single solute in water.

3.1 Hydration structure around single solute

We present here results of our MD simulation on the hydration structure around a single flat planar solute of various sizes with two types of solute–solvent interaction, namely a LJ interaction with parameters chosen from a force field that is commonly used in bio molecular simulations and a purely repulsive counter part of the same potential obtained using WCA approximation [42]. In figure 2, we show the results for the density profile around the solute with LJ interactions for three different sizes of the solute. The density profile in all the cases in this study have been computed from the simulation trajectory by considering a rectangular slab around the solute with the x- and y-dimensions of the slab taken as same as those of the solute plate and the z-dimension is the same as the simulation box length in the z-direction. The nature of the density profiles in all the three cases is quite similar to each other with a large first peak showing a much higher density in the first solvation shell compared to the same in the bulk. The second peak in the density profile that arises due to the solvent structure in the second solvation shell for each of the three solutes is also very prominent. Thus in all the three solute sizes considered here we find profound wetting. Moreover, the heights of the first peaks in the density profiles around all the three solutes are almost the same. In fact, a closer look reveals that it slightly increases with increasing sizes of the solute.

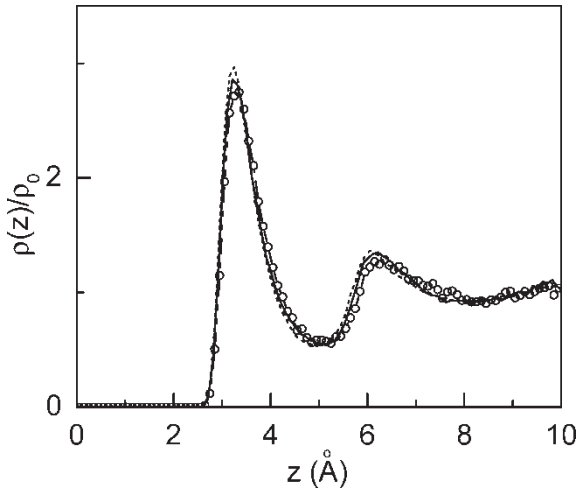

Figure 2. Plot of the normalized single particle density $\rho(z)/\rho_0$ of water oxygen as a function of z, the distance perpendicular to the solute plate with LJ interaction for three different sizes; half of the box is shown. The smallest one with 7 Å × 7 Å dimension is shown by open circle with line, medium one with 11 Å × 12 Å dimension is shown by solid line and the largest one with 20 Å × 20 Å dimension is shown by dashed line.

The negligible effect of the solute size on the hydration water structure can be attributed to a collective or cumulative effect of a large number of small attractions between water molecule and the individual carbon atoms of the solute.

In figure 3, we show the density profiles for the three solutes with same sizes and geometry as above, but solute potentials are represented in all the three cases by a purely repulsive interaction as obtained from the WCA decomposition of the above mentioned LJ interaction. The nature of density profiles in this case is distinctly different from the same of their LJ counter parts. There is no strong layering around the solute as compared to their LJ analogue, which is highly hydrated as indicated by the profound peaks and troughs in the density profile

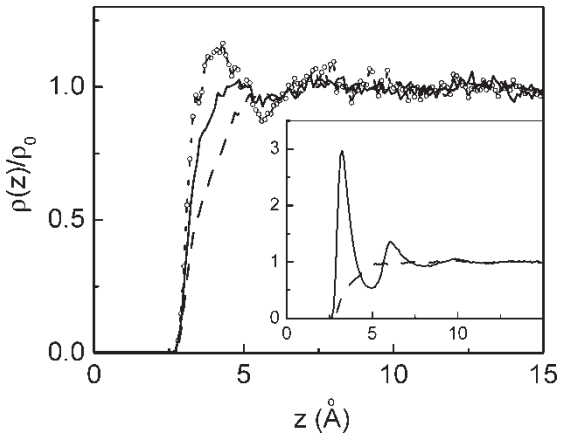

Figure 3. Same as figure 2 but the potential of the solute atoms modeled as purely repulsive part of the LJ interaction as obtained from WCA approximation. The legends are the same as in figure 2. In the inset the density Profile of water around the largest solute with a purely repulsive interaction (dashed line) is compared with the same with LJ interaction (solid line).

(compare figures 1 and 2). In case of a repulsive solute no significant second peak in the density profile has been observed for any of the solutes [19]. Most importantly, we observe a strong solute size dependence of the water accumulation around the purely repulsive solutes in sharp contrast to their LJ analogues. The peak heights in the density profiles decreases with increasing sizes of the solutes. The largest solute plate considered here is around 20Å × 20 Å and the first peak in the density profile in this case does not cross the bulk value until well past contact. In the inset of figure 3, we show the density profiles around the largest solute considered in this study with and without attractive solute–solvent interactions. It clearly shows that the whole shape and nature of the density profiles in this two cases are quite different.

As already discussed the attractive forces among the fluid molecules near a large repulsive solute surface are unbalanced [37], which in effect causes an effective repulsion (CEP [24]) to arise between the fluid and solute surface. Due to the CEP, fluid density near a large completely repulsive solute is suppressed as compared to that of a purely repulsive solvent (with the same excluded volume) around the same solute. It is expected that with increase in the solute size the CEP will increase as more imbalance in attractive forces of water is developed near larger solute surface. Thus, we observe decreasing density peaks with increasing solute sizes for purely repulsive models.

However, when an attractive dispersion interaction is introduced into the solute–water interaction potential, the cumulative attractive interaction between the solute and the solvent compensates for this cavity expulsion potential and therefore we observe a significant hydration of the nanoscopic solutes. The amount of attraction generated from the interactions of all the solute atoms with water, even for the smallest solute considered in this study, is sufficient to offset the CEP and a higher density of water in the first solvation shell as compared to the same of the bulk results. With the increase in solute size as the CEP and the solute–solvent attraction act in the opposite direction, the two opposing effects nullify each other in case of medium and large solutes considered here. To be more explicit, the CEP tries to depress the solvent density around larger solutes where as the attractive solute–solvent interaction enhances it making the density of water in the first solvation shell for all the three different sized attractive solutes nearly the same.

The physically natural dispersion interaction is a natural determinant in the wetting/dewetting behavior of a nanoscopic hydrophobic solute. The LJ interaction depth in the present study is taken from one of the popular force fields and comparison of this value with the same from other force fields as shown in row one of table 1 shows that they are not very different from each other. The precise value of this problematic parameter, from the stand point of quantum chemistry, is not known; the dispersion for a real graphene–water system is not easily quantified either.

Table 1. Non-bonded parameters for atoms in various group that constitute the hydrophobic side chains of amino acids in a protein.

	ϵ (kcal mol^{-1})		
Atom, Group	*AMBER*[*]	*CHARMM*[†]	*OPLS-AA*[‡]
C, sp^2 (aromatic)	0.0860	0.0700	0.0700
C, R-CH3 (sp^3)	0.1094	0.0800	0.0660
C, R$_2$-CH2 (sp^3)	0.1094	0.0550	0.0660
C, R$_3$-CH (sp^3)	0.1094	0.0200	0.0660

[*] Taken from Cornell, W.D. *et al.* (1995) *J. Am. Chem. Soc.* **117**, 5179. [†] Taken from MacKerell Jr., A.D. *et al.* (1998) *J. Phys. Chem. B* **102**, 3586. [‡] Taken from Jorgensen, W.L. *et al.* (1996) *J. Am. Chem. Soc.* **118**, 11225.

3.2 Hydration structure of two-solutes system

We have discussed above how the hydration behavior of a hydrophobic nanoscopic solute with a realistic dispersion interactions with the solvent may be different from that of a geometrically identical solute with a purely repulsive solute–solvent interaction. In this section we investigate the role of solute–solvent attraction on the wetting/dewetting behavior of the inter solute region between two nanoscopic solute plates of 11 Å × 12 Å dimension. As discussed in the beginning of this section, in our earlier work we found a monolayer of water between the two solute plates with the well depth of the solute–solvent LJ interaction at 0.086 kcal mol^{-1}. As the same carbon parameters from other force fields are not very different (see Table 1), we can expect this feature to be relatively insensitive to our choice of the force field. The question of obtaining an accurate interaction potential of water with graphene is technically much more challenging and we do not address that here. However this free energy minimum and the corresponding monolayer state is not seen when a purely repulsive solute is considered. Here we report how the inter solute wetting/dewetting behavior depends on the mean field solute–solvent attraction using simple classical potentials.

In figure 4, we have shown the density profiles for the four cases corresponding to system A, B, C and D as defined above. There are two aspects to be noticed here: the water structure in the inter solute region and that in the vicinity of the outer side of each plate. For systems A and B where the LJ interaction parameter ϵ for individual solute atoms are 0.086 kcal mol^{-1} and 0.052 kcal mol^{-1}, the inter solute region contains a monolayer as indicated by the appearance of a sharp peak in the water density in the middle of the two solute plates. When the LJ interaction parameter ϵ is reduced to 0.023 kcal mol^{-1} we observe an expelling of the majority of the water molecules from the inter solute region consistent with the presence of a very small peak in this region. If we look at the density peak just outside of the two plates, in all the above three cases (systems A–C) we observe a much higher water density as compared to bulk, indicating wetting of the outer surfaces. Thus a substantial density depression in the inter solute region for system C is the combined effect of the two large plates and the interaction parameters chosen.

Thus the wetting/dewetting behavior in the inter solute region is quite different from that for an individual solute or on the exterior of a solute system. Finally, for purely repulsive interactions (system D), which we obtained from a WCA decomposition of the full LJ potential in system A, we observe almost a complete dewetting. In this case, there is no density peak in the middle and more importantly the water structure on the outside of the solute surface is also significantly diminished indicating

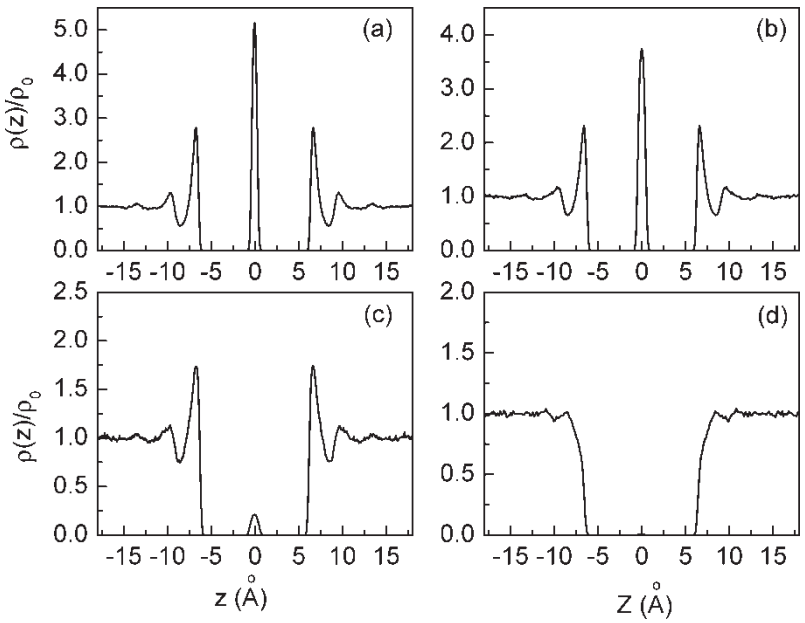

Figure 4. Plot of the normalized single particle density $\rho(z)/\rho_0$ of water oxygen around two plates of dimension 11 Å × 12 Å as a function of z, the distance perpendicular to the solute plates with a fixed inter solute distance of 6.8 Å for four different potential parameters: (a) System A, (b) System B, (c) System C and (d) System D (see text for definition).

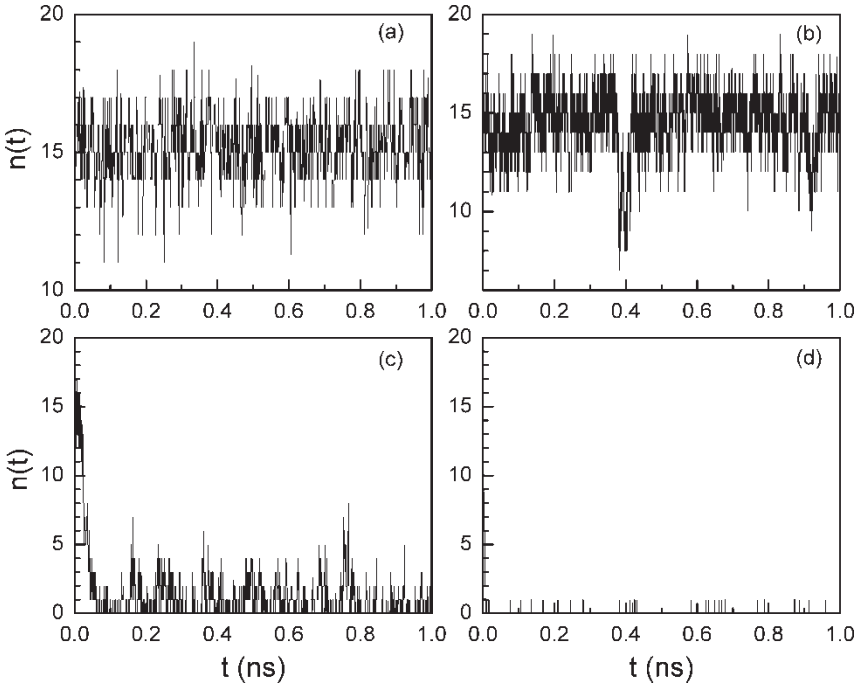

Figure 5. Plot of the number of confined water molecules $n(t)$ between the two plates vs time in nano seconds for the total simulation time of 1 ns corresponding to the four cases of figure 4. i.e. for: (a) System A, (b) System B, (c) System C and (d) System D.

that water molecules are not attracted to the surface but still retain a subtle layering as noted previously by Rossky *et al.* [19] and evidenced in the angular distributions.

The density profile presented is a time averaged quantity and thus does not give us the instantaneous view of the water occupancy in the inter solute region, which might be important if fluctuations are large. We have calculated the instantaneous number of water molecules $n(t)$ in the inter solute region as a function of time t for a period of 1 ns of simulation time for each of the four systems considered here. These are shown in figure 5. We observe that for system A and B we have around 12–17 water molecules through out the entire simulation period of 1 ns. For system C although simulation was started with around 16 inter solute water molecules, within 60 ps almost 10–12 water molecules were expelled leaving behind 0 to 4 water molecules for the rest of the simulation time. For the repulsive solute case (system D) the inter solute region dewets within 10–20 ps and we find almost no water (0 or 1 water molecule) for the entire simulation time. If we look at the energy parameters ϵs for various atoms in various hydrophobic side chains of a protein as listed in Table 1, it is found that ϵs for most of the groups such as CH_2, CH_3, aromatic carbon etc. lie in the range of 0.05 kcal mol^{-1} that corresponds to the energy parameter of the solute atoms in system B and above.

4. Conclusions

Various aspects of the hydration structure of water around a single hydrophobic solute as well as in between two solutes have been considered here. The effects of solute size and solute–solvent attraction on the hydration behavior of hydrophobic solutes have been investigated. In case of purely repulsive model solutes, the density of water in the first solvation shell depends strongly on the size of the solute. For the smallest sized solute considered here, we found the water density in the first solvation shell is above that in bulk water. However, a pronounced size effect, which shows increasing density depression with increasing size, has been observed in the purely repulsive case. For commonly used LJ interactions for the carbon atoms of the solute, however, we found a considerably larger water density in the first solvation shell of the solute that does not change with the change in the sizes of the solute plates. The gain in energy from the cumulative attractive interactions between the solute atoms and the solvent, given a layered distribution (See figure 1), compensates for the loss due to breaking of the hydrogen bonds in water.

Also the role of solute–solvent interaction on the inter solute solvation, which is very important for the inter solute dewetting and hydrophobic association, has been clearly demonstrated. For moderate solute–solvent attraction of the range of 0.05 kcal mol^{-1} and above, in which range well depths of most of the hydrophobic groups from various modern force fields lie, no dewetting is observed. It is interesting to observe that even when the inter solute region shows the beginnings of a drying transition at a sufficiently small solute well depth of 0.023 kcal mol^{-1}, the outer surfaces of the solute still remain substantially hydrated. This shows the concerted effect of two solutes with insufficient attractions force the water to leave the inter solute region. Dewetting behavior

of the inter solute region thus may not always be predictable in a simple straightforward fashion from the hydration behavior of a single solute.

Acknowledgements

We gratefully acknowledge NIH, the R.A. Welch foundation, and TIMES, funded by NASA Cooperative Agreement No. NC-1-02038 for partial financial support of this work. The computations were performed in part using the NSF meta center facilities and the Molecular Science Computing Facility in the W.R. Wiley Environmental Molecular Sciences Laboratory, a national scientific user facility sponsored by DOE's Office of Biological and Environmental Research and located at Pacific Northwest National Laboratory, operated for DOE by Battelle.

References

[1] W. Kauzmann. Some factors in the interpretation of protein denaturation. *Adv. Protein Chem.*, **14**, 1 (1959).
[2] L.R. Pratt, A. Pohorille. Hydrophobic effects and modelling of biophysical aqueous solution interfaces. *Chem. Rev.*, **102**, 2671 (2002).
[3] C. Tanford. *The Hydrophobic Effect: Formation of Micelles and Biological Membranes*, John Weiley, New York (1973).
[4] K.A. Dill. Dominant forces in protein folding. *Biochemistry*, **29**, 7133 (1990).
[5] C. Tanford. How protein chemists learned about the hydrophobic factor. *Protein Sci.*, **6**, 1358 (1997).
[6] C. Tanford. The hydrophobic effect and the organization of living matter. *Science*, **200**, 1012 (1978).
[7] C.L. Brooks, J.N. Onuchic, D.J. Wales. Taking a walk on a landscape. *Science*, **293**, 612 (2001).
[8] J. Shea, C.L. Brooks. From folding theories to folding proteins: A review and assessment of simulation studies of protein folding and unfolding. *Annu. Rev. Phys. Chem.*, **52**, 499 (2001).
[9] G. Hummer, S. Garde, A.E. Garcia, L.R. Pratt. New perspectives on hydrophobic effects. *Chem. Phys.*, **258**, 349–370 (2000).
[10] L. Lu, M.L. Berkowitz. Molecular dynamics simulation of a reverse micelle self assembly in supercritical CO_2. *J. Am. Chem. Soc.*, **126**, 10254 (2004).
[11] S. Niyogi, R.C. Haddon. Behavior of fluids in nanoscopic space. *Proc. Natl Acad. Sci.*, **101**, 6331 (2004).
[12] N. Chakrapani, B. Wei, A. Carrillo, P.M. Ajayan, R.S. Kane. Capillarity-driven assembly of two-dimensional cellular carbon nanotube foams. *Proc. Natl Acad. Sci.*, **101**, 4009 (2004).
[13] C.A. Angel. *Water: A Comprehensive Treatise*, F. Franks (Ed.), Vol. 7, pp. 1–81, Plenum, New York (1982).
[14] K. Lum, D. Chandler, J.D. Weeks. Hydrophobicity at small and large length scales. *J. Phys. Chem. B*, **103**, 4570 (1999).
[15] C. Pangali, M. Rao, B.J. Berne. A Monte Carlo simulation of the hydrophobic interaction. *J. Chem. Phys.*, **71**, 2975 (1979).
[16] D.E. Smith, A.D.J. Haymet. Free energy, entropy, and internal energy of hydrophobic interactions: Computer simulations. *J. Chem. Phys.*, **98**, 6445 (1993).
[17] G. Hummer, S. Garde, A.E. Garcia, A. Pohorille, L.R. Pratt. An information theory model of hydrophobic interactions. *Proc. Natl. Acad. Sci. USA*, **93**, 8951 (1996).
[18] N.T. Southall, K.A. Dill. Potential of mean force between two hydrophobic solutes in water. *Biophys. Chem.*, **101**, 295 (2002).
[19] C.Y. Lee, J.A. McCammon, P.J. Rossky. The structure of liquid water at an extended hydrophobic surface. *J. Chem. Phys.*, **80**, 4448 (1984).
[20] S.H. Lee, P.J. Rossky. A comparison of the structure and dynamics of liquid water at hydrophobic and hydrophilic surfaces a molecular dynamics simulation study. *J. Chem. Phys.*, **100**, 3334 (1994).
[21] D.M. Huang, D. Chandler. Temperature and length scale dependence of hydrophobic effects and their possible implications for protein folding. *Proc. Natl Acad. Sci. USA*, **97**, 8324 (2000).
[22] D.M. Huang, D. Chandler. The hydrophobic effect and the influence of solute–solvent attractions. *J. Phys. Chem. B*, **106**, 2047 (2002).
[23] Rein, P. ten Wolde, D. Chandler. Drying-induced hydrophobic polymer collapse. *Proc. Natl Acad. Sci. USA*, **99**, 6539 (2002).
[24] G. Hummer, S. Garde. Cavity expulsion and weak dewetting of hydrophobic solutes in water. *Phys. Rev. Lett.*, **80**, 4193 (1998).
[25] A. Wallqvist, B.J. Berne. Molecular dynamics study of the dependence of water solvation free energy on solute curvature and surface area. *J. Phys. Chem.*, **99**, 2893 (1995).
[26] X. Huang, C.J. Margulis, B.J. Berne. Dewetting-induced collapse of hydrophobic particles. *Proc. Natl Acad. Sci. USA*, **100**, 11953 (2003).
[27] G. Hummer, J.C. Rasaiah, J.P. Noworyta. Water conduction through the hydrophobic channel of a carbon nanotube. *Nature*, **414**, 188 (2001).
[28] M.S.P. Sansom, P.C. Biggin. Water at the nanoscale. *Nature*, **414**, 156 (2001).
[29] A. Kalra, S. Garde, G. Hummer. Osmotic water transport through carbon nanotube membranes. *Proc. Natl Acad. Sci. USA*, **100**, 10175 (2003).
[30] J.L. Parker, P.M. Claesson, P. Attard. Bubbles, cavities, and the long-ranged attraction between hydrophobic surfaces. *J. Phys. Chem.*, **98**, 8468 (1994).
[31] R.M. Pashley, P.M. McGuiggan, B.W. Ninham, D.F. Evans. Attractive forces between uncharged hydrophobic surfaces: Direct measurements in aqueous solution. *Science*, **229**, 1088 (1985).
[32] R. Steitz, T. Gutberlet, T. Hauss, B. Klosgen, R. Krastev, S. Schemmel, A.C. Simonsen, G.H. Findenegg. Nanobubbles and their precursor layer at the interface of water against a hydrophobic substrate. *Langmuir*, **19**, 2409 (2003).
[33] T.R. Jensen, M.O. Jensen, N. Reitzel, K. Balashev, G.H. Peters, K. Kjaer, T. Bjorn-holm. Water in contact with extended hydrophobic surfaces: direct evidence of weak dewetting. *Phys. Rev. Lett.*, **90**, 086101 (2003).
[34] D. Schwendel, T. Hayashi, R. Dahint, A. Pertsin, M. Grunze, R. Steitz, F. Schreiber. Interaction of water with self-assembled monolayers: Neutron reflectivity measurements of the water density in the interface region. *Langmuir*, **19**, 2284 (2003).
[35] P. Ball. How to keep dry in water. *Nature*, **423**, 25 (2003).
[36] A. Walqvist, E. Gallicchio, R.M. Levy. A model for studying drying at hydrophobic interfaces: Structural and thermodynamic properties. *J. Phys. Chem.*, **105**, 6745–6753 (2001).
[37] H.S. Ashbaug, M.E. Paulaitis. Effect of solute size and solute-water attractive interactions on hydration water structure around hydrophobic solutes. *J. Am. Chem. Soc.*, **123**, 10721–10728 (2001).
[38] N. Choudhury, B.M. Pettitt. On the mechanism of hydrophobic association of nanoscopic solutes. *J. Am. Chem. Soc.*, (2004) (Accepted).
[39] Y.M. Rhee, E.J. Sorin, G. Jayachandran, E. Lindahl, S. Pande. Simulations of the role of water in the protein-folding mechanism. *Proc. Natl Acad. Sci. USA*, **101**, 6456 (2004).
[40] H.J.C. Berendsen, J.R. Grigera, T.P. Straatsma. The missing term in effective pair potentials. *J. Phys. Chem.*, **91**, 6269 (1987).
[41] D.W. Cornell, W.D. Cornell, P. Cieplak, C.I. Bayly, I.R. Gould, K.M. Merz, D.M. Ferguson, D.C. Spellmeyer, T. Fox, J.W. Caldwell, P.A. Kollman. A second generation force field for the simulation of proteins, nucleic acids, and organic molecules. *J. Am. Chem. Soc.*, **117**, 5179 (1995).
[42] D. Chandler, J.D. Weeks, H.C. Andersen. Van der Waals picture of liquids, solids, and phase transformations. *Science*, **220**, 787 (1983).
[43] S. Nose. A Molecular dynamics method for simulation in the canonical ensemble. *Mol. Phys.*, **100**, 191 (2002).
[44] H.C. Andersen. Molecular dynamics simulations at constant pressure and/or temperature. *J. Chem. Phys.*, **72**, 2384 (1980).
[45] S. Nose, M.L. Klein. Constant pressure molecular dynamics for molecular systems. *Mol. Phys.*, **50**, 1055 (1983).
[46] M.P. Allen, D.J. Tildesley. *Computer Simulation of Liquids*, Oxford University, New York (1987).
[47] H.C. Andersen. Rattle: A "velocity" version of the shake algorithm for molecular dynamics calculations. *J. Comput. Phys.*, **52**, 24 (1983).
[48] W.C. Swope, H.C. Andersen, P.H. Berens, K.R. Wilson. A computer simulation method for the calculation of equilibrium constants for the formation of physical clusters of molecules: Application to small water clusters. *J. Chem. Phys.*, **76**, 637 (1982).
[49] D. Leckband, J. Israelachvili. Intermolecular forces in biology. *Q. Rev. Bio-Physics*, **34**, 105 (2001).